Calibration of the Scanning Kelvin Probe Force Microscope under Controlled Environmental Conditions

A. B. Cook[1], Z. Barrett[2], S. B. Lyon[3], H. N. McMurray[2], J. Walton[3] and G. Williams[2]

[1]Materials Performance Centre, School of Materials, The University of Manchester, Sackville Street, Manchester M13 9PL, UK

[2]Materials Research Centre, College of Engineering, Swansea University, Singleton Park, Swansea SA2 8PP, Wales, UK.

[3]Corrosion and Protection Centre, School of Materials, The University of Manchester, Sackville Street, Manchester M13 9PL, UK

Abstract

Local Volta potential differences ($\Delta\psi$) between a platinum coated AFM tip and various pure metal specimens with a thin humidity induced surface electrolyte layer have been determined via scanning Kelvin probe force microscopy (SKPFM). SKPFM determined $\Delta\psi$ display a linear correlation with the same quantities determined under nominally identical environmental conditions using a scanning Kelvin probe (SKP); the slope is within experimental error one. By exploiting this correlation and using a SKP previously calibrated versus a series of metal/aqueous metal ion redox couples it is possible to indirectly calibrate atmospheric SKPFM derived $\Delta\psi$ with electrochemical potential. Good correlation is also obtained between immersion corrosion potential (E_{corr}) in NaCl electrolyte and SKP derived $\Delta\psi$ in the presence of a NaCl dosed humidity layer. This implies that SKPFM may be calibrated directly against immersion E_{corr} provided SKPFM measurements are performed under suitably controlled conditions of atmospheric relative humidity and surface electrolyte dosing.

Introduction

The Kelvin probe (KP) was first applied in applications pertaining to corrosion science by Stratmann and co-workers who presented the theory, working principles and application of the technique in a series of landmark publications [1-4]. It was shown that the local Volta potential difference ($\Delta\psi$) between a probe vibrated above a specimen with a thin electrolyte layer on the surface varied linearly with corrosion potential (E_{corr}) as measured versus a standard reference electrode. As such the calibrated KP provided a means of determining E_{corr} beneath thin electrolyte layers. Since that time the scanning Kelvin probe technique (SKP) has found widespread application, proving an invaluable tool, in kinetic and mechanistic study of atmospheric corrosion processes under thin and ultrathin electrolyte layers [5,6] and polymeric coatings [7-12]. In regards to corrosion in the latter condition it has been particularly useful in experimental studies regarding inhibition of corrosion driven delamination with pigmented coatings containing chromate [13,14], rare and alkaline earth [15,16], hydrotalcite [17-19] and polyaniline species [20-23].

Scanning Kelvin probe force microscopy (SKPFM), an AFM variant of the SKP technique provides a fundamentally different means of measuring $\Delta\psi$. Both SKP and SKPFM are nulling techniques but in the latter it is a component of a force induced via the coupling of an imposed AC field and the contact potential difference set up on bringing the probe and specimen into electronic contact, rather than an induced AC current, that is nulled. As such high AC fields exist between tip and specimen during measurement that may affect the value of potentials determined for specimens that form semi-conducting surface layers, as has been demonstrated experimentally [24]. $\Delta\psi$ values derived via the technique are also subject to contributions to the capacity gradient between tip and specimen from surface topography and other surface

heterogeneities. Indeed as stated by Jacob's et al. [25] potentials measured via SKPFM are influenced by all surface elements of the tip and specimen. In general the SKPFM is found to measure significantly lower potential contrast on heterogeneous surfaces than SKP. A discussion artefacts associated with SKPFM, their origins and effects has been provided by Rohwerder and Turcu [26].

In terms of its use in corrosion science SKPFM, was introduced ca. a decade after SKP by Schmutz and Frankel [27] who found that the Volta potentials measured on a range of pure metals upon their emersion from NaCl and de-ionised water displayed a linear relationship with E_{corr} values measured during immersion in such aqueous environments. As a result it was suggested that $\Delta\psi$ measured in air provides a measure of the local practical nobility and it was indeed demonstrated that values for Cu containing intermetallics in polished Al 2024 are noble to that of the matrix [27]. This is in agreement with trends in E_{corr} values observed in NaCl solution [28]. Since the work of Schmutz and Frankel many other researchers have used Volta potential differences determined by SKPFM in air to characterize alloy surfaces and as such predict the likely localized corrosion behaviour of various alloy systems in solution [29-36]. A discussion of the pitfalls that may be encountered in simply extrapolating the findings of Frankel et al. to other alloy systems, i.e. using $\Delta\psi$ measured on freshly polished surfaces to predict subsequent behaviour in solution may be found in the aforementioned article by Rohwerder and Turcu [26]. The technique has also been used for in-situ corrosion studies; for example coating delamination on the sub-micrometer scale [37] and in investigating the atmospheric corrosion of magnesium alloys in CO_2 containing humid air [38].

Given the self-evident desirability of being able to extract local E_{corr} values from SKPFM data we have sought to establish a rigorous demonstration of SKPFM

calibration in terms of E_{corr} under controlled atmospheric conditions of known humidity. In so doing we have made use of the fact that a well established method already exists for the calibration of macroscopic SKP [10,13]. In the current paper we use a calibrated SKP to determine atmospheric E_{corr} values on various notionally pure metals covered by a thin aqueous surface layer produced by water adsorption from air at *ca* 80%RH. This has been done in both the presence and absence of electrolyte (salt) dosing in the aqueous surface layer. We also use SKPFM to determine $\Delta\psi$ values for the same surfaces. A correlation of SKPFM derived $\Delta\psi$ values with E_{corr} values derived from calibrated SKP then allows an unequivocal calibration of SKPFM in terms of E_{corr}. To our knowledge this is the first time that such a calibration has been performed under controlled environmental conditions. Our findings also tend to support the general validity of the approach to calibration employed by Schmutz and Frankel [27].

Background to SKP and SKPFM techniques

SKP. – The theory behind this technique has been discussed in detail elsewhere [10,13,39]. In brief it provides a means of determining $\Delta\psi$ between a specimen and reference probe with a resolution of ca. 100 μm. In the presence of a thin electrolyte layer [2,13] the potential difference measured by SKP (E_{kp}) is the local Volta potential difference between the probe and specimen, $\Delta\psi_{sol}^{probe}$. This quantity has been shown to be related to E_{corr} via

$$E_{corr} = \left(E_{ref} + \frac{\phi^{probe}}{F} - \chi_{gas}^{sol} \right) + \Delta\psi_{sol}^{probe} = B + \Delta\psi_{sol}^{probe} \qquad (1)$$

where E_{ref} is the absolute half-cell potential of the SHE, ϕ^{probe} the electronic work function of the reference probe, F the Faraday constant and χ_{gas}^{sol} the surface potential of the solution/gas interface. Since E_{ref}, F and ϕ^{probe} are constants and χ_{gas}^{sol} is small and constant for a given electrolyte [40] then, as has been demonstrated many times experimentally, $\Delta\psi_{sol}^{probe}$ varies linearly with E_{corr}.

SKPFM. – This technique involves the measurement of topography and contact potential difference sequentially on a line by line basis in a two-pass measurement with an AFM [41]. Firstly specimen topography is determined along the analysis line in conventional tapping mode, the probe moved to a pre-determined lift-height (typically ca. 100 nm [27]) and rescanned above the surface following the previously determined topographic profile. In determining $\Delta\psi$ the tapping piezo is disabled and an AC signal at the resonant frequency of the cantilever (ω) applied to the tip. At this frequency the AC signal induces mechanical oscillation in the cantilever as a result of an oscillating electrical force (F_e) that arises via its coupling with the DC contact potential difference produced due to the Fermi level alignment on bringing the tip and specimen into electronic contact. F_e is related to the rate of change of energy across the capacitor formed between the probe and the specimen by:

$$F_e = -\frac{dW_{cap}}{dz} = \frac{1}{2}V^2\frac{dC}{dz} \qquad (2)$$

Where, W_{cap}, is the energy stored in the capacitor formed between tip and specimen, V, the potential difference across this capacitor, C the capacitance and z the probe to

specimen separation distance. With $V = V_{dc} + V_{ac} \sin \omega t$, and $2\sin^2 x = \frac{1}{2}(1 - 2\cos x)$ equation 2 becomes:

$$F_e = \frac{1}{2}\frac{dC}{dz}(V_{dc}^2 + \frac{1}{2}V_{ac}^2) - \frac{dC}{dz}V_{dc}V_{ac}\sin(\omega t) + \frac{1}{4}\frac{dC}{dz}V_{ac}^2\cos(2\omega t) \quad (3)$$

where V_{dc} and V_{ac} are the DC contact potential difference and amplitude of the AC signal, respectively. The force component of F_e at ω becomes zero when V_{dc} is zero. Under such conditions the frequency of F_e is 2ω and as the mechanical vibration induced in the cantilever at this frequency is effectively zero there is no significant mechanical oscillation of the probe. In practice, therefore, the condition V_{dc} = 0 is achieved by applying to the tip a DC voltage that nulls the mechanical oscillation. If contributions to the capacitance from the cantilever, surface artefacts and the sides of the probe are assumed to be negligible then the DC voltage required to achieve the null condition is, for a specimen covered with a thin electrolyte layer, equal to the Volta potential difference between the electrolyte and the probe ($\Delta\psi_{probe}^{electrolyte}$); this is of opposite sign to E_{kp}. Hence in principle the potential difference determined via SKPFM (E_{skpfm}) provides on inversion a measure of $\Delta\psi_{electrolyte}^{probe}$ on a sub-micrometer scale.

Experimental

Materials/specimen preparation. – All metals (Ag, Zn, Cu, Ni and Fe) were obtained from Goodfellow Metals Cambridge as 1 mm thick sheet with purity 99.99%+. All metal salts were of ACS reagent grade and obtained from either BDH or the Aldrich

Chemical Company. Solutions were prepared using either de-ionised water or, in the case of those used for surface electrolyte dosing, methanol (Fisher Scientific, 99.9%+). SKP and SKPFM experiments were performed on 25 and 10 mm square metal coupons, respectively, wet polished to 4000 grit with SiC paper, degreased with ethanol and dried under a stream of cold air. The metal surfaces thus prepared were either exposed directly to the humid atmosphere of the SKP/SKPFM chamber or, when required, first dosed with a small quantity of NaCl (or $AgNO_3$ in the case of Ag) by emersing the coupon from a 0.05 mol dm^{-3} methanolic solution of the relevant salt. The emersed coupons were then held in room air for *ca* 20 minutes to produce a finely dispersed, and nominally dry, salt deposit. On coupons intended for SKP measurements electrolyte dosing was typically performed on one half of the metal coupon so that the adsorbed humidity layer subsequently forming on that half of the coupon in the SKP chamber would comprise electrolyte, whilst the other half would comprise notionally pure water. Thus by scanning from one half of the coupon to the other the influence of electrolyte on atmospheric E_{corr} values could be obtained from a single coupon in a single experiment.

Methods. – The SKP instrument used in this work incorporated a 125 μm diameter Au wire as the reference probe vibrated at 280 Hz at an average probe to sample height of 100 μm with 40 μm amplitude. Details of its design and the methodology used to determine the constant *B* in equation 1 and subsequent evaluation of E_{corr} values in the presence of thin electrolyte films has been described in detail elsewhere [2,13,42]. All experimental SKP measurements were conducted at ambient temperature (nominally 25^{o}C) with a 5% w/v aqueous NaCl humidity reference solution present in the SKP sample chamber. Time-dependent chamber RH was monitored continually in real

time with a Lascar USB temperature and humidity sensor (EL-USB-2-LCD). On closing the chamber RH was found to rise monotonically from its ambient value (nominally 50%) to approximately 96% (equilibrium value predicted from water activity in reference solution) and reached 80% approximately one hour following closure of the chamber. E_{corr} values were found to be substantially RH independent over the range 80% to 96% RH and all the values subsequently reported herein were recorded with the RH in this range (i.e. 80% - 96%RH). At 80% RH NaCl wets to form a thin near-saturated electrolyte layer; the deliquescence point of NaCl is 76% at 25°C [42]. One hour after sealing the environmental chamber, the reference probe of the SKP was scanned over a 7.95 mm line across the nominal electrolyte/electrolyte interface with 20 data points per millimetre. Twelve scans were conducted consecutively each taking five minutes to complete; at the end of each scan the probe was re-configured immediately and the area rescanned. During scanning the RH was not observed to rise significantly above 80% and E_{kp} values were substantially time-independent. The E_{kp} value used for correlation with the potential measured under identical conditions via SKPFM is the average from all twelve scans.

SKPFM measurements were performed using a Nanoscope III Multimode AFM equipped with an Extender Electronics Module (Bruker). Pt coated Si cantilevers with resonant frequency between 45 and 95 kHz (Bruker OSCM-PT) were used in all experiments. Control of the instrument and data acquisition was achieved via Nanoscope ® III Version 5.12r3. To allow measurement of the maximum potential contrast the option in the software for addition of a plane fit was disabled. The microscope was fitted with a transparent environmental hood (Bruker MMAHC-201) to allow control of the RH. The environmental conditions were the same as for SKP measurement but RH control was in this case accomplished by the passage of

humidified air through the chamber. Humidification of the air was achieved by passing a stream of air through five Dreschel bottles containing 5% NaCl prior to its entry into the chamber. The first of these bottles was thermostated at 65°C by placing it in a water bath; the other four were kept at ambient temperature. Temperature and RH was monitored in real time as described previously. This method of humidity control resulted in a steady RH of 80% being achieved rather than the expected value of 96% (the equilibrium RH above 5% NaCl). Hence all SKP and SKPFM experiments were performed when the environmental RH reached 80%.

SKPFM measurements were made, as previously described, in the presence of a thin aqueous humidity layer formed through water adsorption at the metal surface from air at 80% RH both in the presence and absence of electrolyte dosing in that humidity layer. Prior to each surface potential measurement a topographic map of an area 16 μm^2 was acquired at 0.4 Hz (scan time 21 minutes) under ambient conditions; ca. 25°C and 30% RH. Topographic and Volta potential difference maps were then procured, at the same scan rate, over a 4 μm^2 section selected from within this region. Volta potential difference maps were obtained at a lift-height of 400 nm with an AC drive amplitude of 5 V at the resonant frequency of the cantilever (ω). The Pt coated probes act as a pseudo reference and some variation in the measured potential were found from tip to tip, but as these differences were small relative to the potentials being measured the E_{skpfm} values reported herein were not referenced to any particular standard. They are however inverted to be consistent with the sign of their associated E_{kp} values. E_{skpfm} values are of opposite sign to E_{kp} values as the potential used to null the DC potential between the tip and specimen is applied to the tip and not to the specimen as in conventional SKP. Image data files were processed using Nanoscope Analysis software version 1.2. E_{skpfm} values used in comparisons with corresponding

E_{kp} were the mean surface potential as determined from the Volta potential difference maps using the surface roughness tool.

Results and Discussion

The influence of electrolyte dosing on atmospheric E_{kp}. – In the absence of electrolyte (salt) dosing the aqueous humidity film forming at the metal-air interface at 80%RH is expected to be only a few molecular layers thick [5]. When NaCl (deliquescence point 76% at 25°C [43].) or $AgNO_3$ are present the humidity films are likely to be thicker. However, in no case was bulk water observed to become visibly condensed on the metal surface. The effect of electrolyte dosing on E_{kp} ($\Delta\psi_{solution}^{probe}$) is illustrated in Figure 1 in the form of a series of SKP line scans. In each case the SKP probe was scanned from the electrolyte dosed to (nominally) electrolyte free area of the relevant metal surface along a line normal to the boundary between the two areas). It may be seen that for Ag and Zn the value of E_{kp} is not greatly influenced by the presence of $AgNO_3$ and NaCl respectively. Conversely, the presence of NaCl is seen to reduce E_{kp} values on Cu and Fe by *ca.* 0.2 and *ca.* 0.4 V respectively.

The simplest explanation for the above findings is that they reflect the tendency of the relevant metal (a) to passivate in humid air and (b) become depassivated and undergo active corrosion in the presence of aggressive electrolyte. Certainly, the drop in E_{kp} observed on both Fe and Cu in the presence of NaCl is immediately consistent with a passive – active transition induced by aggressive Cl^- anions. The failure to observe a similar drop on Zn was unexpected given multiple reports in the literature that E_{kp} on zinc falls significantly on contact with an activating electrolyte [9,12,20,44]. However, it should be noted that the Zn sample used here was high purity and high purity Zn is known to be a very inactive oxygen reduction

cathode [45]. Consequently, the failure to observe any Cl^- induced passive – active transition probably reflects a correspondingly minimal tendency for high purity Zn to reach high potentials through atmospheric O_2 reduction. However, it should also be noted that for freshly prepared samples (which is the case here) very low passive potentials are sometimes observed when the Fermi level in the oxide is just below the conduction band edge [46]. In the case of Ag it is less likely that NO_3^- ions would act aggressively and the small increase in E_{kp} (ca 0.05 V) actually observed in the $AgNO_3$ dosed area probably reflects the increased local activity of Ag^+.

On the basis of the above it seems reasonable to assume that for Fe, Zn and Cu the atmospheric E_{kp} values recorded in the presence of NaCl dosing reflect, and therefore may be calibrated in terms of, active E_{corr} values for these metals. In the case of Ag it is not possible to exploit Cl^- induced activation because of the insolubility of AgCl. However, the E_{kp} value recorded after $AgNO_3$ dosing probably reflects the potential of the Ag^+/Ag couple. These hypothesis are borne out in curve (ii) in Figure 2 which shows area averaged atmospheric E_{kp} values obtained from the various electrolyte dosed metal surfaces plotted against E_{corr} for the same metals recorded (versus SCE) in the presence of a 2 mm thick electrolyte layer of 5% NaCl (0.5 mol dm^{-3} $AgNO_3$in the case of Ag). The slope and intercept of curve (ii), as obtained by linear regression, are included in Figure 2 and it may be seen that curve (ii) is, within experimental error, a straight line with a slope of 1.

The SKP was also subject to calibration using a well established literature method [13,21] in which E_{corr} (versus SCE) and E_{kp} ($\Delta\psi_{solution}^{probe}$) were measured simultaneously for $Zn/ZnCl_2$, $Fe/FeCl_2$, $Cu/CuCl_2$ and $Ag/AgNO_3$ couples (metal in contact with a 2mm layer of a 0.5 mol dm^{-3} solution of the relevant metal ion). The calibration plot of E_{corr} versus E_{kp} is shown in curve (i) of Figure 2 and is again,

within experimental error, a straight line with a slope of 1. The values for the constant B in equation 1 determined from intercepts of curves (i) and (ii) are 0.294 V and 0.286 V, respectively. The close similarity of curves (i) and (ii) tend to support the notion that the approach to SKPFM calibration used by Schmutz and Frankel [27] was basically valid, at least when the calibration specimens were emersed from aqueous NaCl.

Optimisation of the SKPFM. – Each time a new probe was inserted into the SKPFM the phase of the reference signal (drive phase) was adjusted to ensure maximum output from the lock-in amplifier of the Extender box. This procedure was performed using a modified version of the method of Jacobs et al [25]. Here, rather than apply a square wave voltage from an external source to the specimen as did Jacob's et al [25], we used a Cu grid pressed into a pure Al disk such that the specimen provided its own source of potential difference. With the SKPFM in open-loop configuration the output of the lock-in (input to the feedback loop), identified as 'phase' in the control software [47], is monitored whilst scanning the tip across the dissimilar metals. The drive phase is then adjusted until the output of the lock-in ('phase') is zero. At this point the drive and deflection signals are exactly 90° out of phase. Subtracting 90° from this value provides the magnitude of the drive phase that provides maximum input into the feedback loop allowing the contact potential difference to be tracked with maximum sensitivity in closed-loop configuration. Typically the optimum drive phase for our set up was ca. -74°. The importance of setting the phase correctly cannot be overstated since, as shown by Jacobs et al. [25], it is difficult to judge the optimum drive phase by comparison of potential images.

Determining the drive amplitude for SKPFM. – Typically an AC drive amplitude of 1 V and lift height of 100 nm is employed in SKPFM. With regards to the former quantity the manufacturer's recommend, in the case of the Multimode with an Extender electronics module that a value below 2 V should not be used [48]. Hence to determine the effect of drive amplitude on SKPFM $\Delta\psi$ values were measured at various drive amplitude on nominally bare Zn and Fe with the Multimode and compared to those determined under identical conditions with a Dimension 3100 (Bruker). The optimum drive phase for the latter instrument was determined using the manufacturer's recommended procedure [49]. E_{skpfm} values measured using the 3100 were independent of drive amplitude whereas those obtained using the multimode showed a slight deviation from a linear dependence above ca. 3 V; the divergence from linearity increased with decreasing voltage below this value. The discrepancy is not metal specific and is believed to be an artefact of the analog phase lock loop of the Extender electronics module. Hence in our work with the Multimode a drive amplitude of 5V was employed. Figure 3 shows a plot of the difference between E_{skpfm} values determined with the Multimode and the Dimension 3100 for Zn and Fe as a function of the applied AC drive voltage.

Correlation of E_{skpfm} and E_{kp}. – Figures 4 and 5 show plots of $-E_{skpfm}$ versus E_{kp} obtained from the various metal coupons at 80% RH in the presence and absence of electrolyte (salt) dosing of the aqueous humidity layer respectively. Again the electrolyte used was NaCl, except for Ag when it was $AgNO_3$. The E_{kp} values represent the average measured across the appropriate portions of the 7.95 mm line scans (as shown in Figure 1) recorded over a one hour period whereas E_{skpfm} values are the average measured over a 4 μm^2 area during a 42 minute period. In both

Figures 4 and 5 the slope of the line is 1 within experimental error, with a small offset which probably reflects the difference in work functions between Au and Pt. The strong correlation of $-E_{skpfm}$ with E_{kp} tends to confirm the notion that SKP and SKPFM are essentially performing the same measurement despite the differences in operating principle. It also tends to confirm the notion that SKPFM should be capable of calibration in terms of electrochemical potentials, and specifically E_{corr}, in a manner entirely similar to SKP. A caveat should be inserted here as the SKP and SKPFM measurements were made in separate geographical locations and so there are likely to have been differences in ambient conditions during measurement. This is unlikely to have significantly influenced our results but it should not go unmentioned.

On the basis of the above the E_{kp} values plotted on the x-axes of Figures 4 and 5 were converted to E_{corr} using the SKP calibration data shown in line (i) of Figure 2. The E_{skpfm} data in Figures 4 and 5 were then replotted against the SKP derived E_{corr} data to produce the E_{corr} calibration curve for SKPFM shown in Figure 6. The calibration curve is, within experimental error, a straight line with a slope of 1 and the corresponding value of B in equation 1 is 0.364. The finding that data derived from metals in contact with both electrolyte dosed and non-dosed humidity layers fall on the same line suggests that electrolyte concentration is not a critical factor provided, of course, that it is the same for both instruments. It also tends to support the general validity of the approach adopted by Schmutz and Frankel [27] who calibrated the SKPFM using nominally dry pure metal specimens previously immersed in NaCl and de-ionized water.

Correlation of $-E_{skpfm}$ with calibrated E_{skp} provides a means of calibrating SKPFM which is robust in that it requires making a minimum number of assumptions. However, it must be recognised that SKP instrumentation will not be available in

many laboratories possessing SKPFM thus limiting the practical utility of the approach. Under these circumstances the very close similarity of curves (i) and (ii) in Figure 2 suggests that SKPFM may be calibrated with minimal error directly against E_{corr} values measured under immersion conditions using a conventional reference electrode. In so doing E_{corr} would be measured for a series of metal standards under conditions of aqueous electrolyte immersion and E_{skpfm} would be measured for the same metal standards under conditions of known humidity (above the electrolyte deliquescence point) in the presence of traces of the same electrolyte. Electrolyte dosing in the aqueous humidity layer could be performed using methanolic emersion as in the current paper or, possibly, by aqueous emersion following the approach of Schmutz and Frankel [27].

The limitations of SKPFM calibration. – It must be noted that all the measurements described in the current paper were performed on physically large, uniform, surfaces of high purity metal. As such they are substantially uninfluenced by factors relating to the finite lateral resolution the SKP and SKPFM techniques. This will not be the case in most real circumstances where SKP and particularly SKPFM are being used to image Volta potential (or E_{corr}) variation over a heterogeneous surface. Failure to take this fact into account may give rise to substantial error in the interpretation of results. In both SKP and SKPFM lateral resolution is intrinsically limited by the spreading of electrostatic countercharge on the sample surface beneath the scanning tip [50]. However, in SKPFM limitations in lateral resolution may also arise from stray capacitance between the sample non-tip areas such as the body of the cantilever and sides of the tip. The E_{skpfm} values are, to quote Jacobs et al [25], ‘always a weighted average and all surface elements of the tip and the sample affect its value’. An

excellent critical discussion of the various artefacts that may affect measurements with the SKPFM has been provided by Rohwerder and Turcu [26]. On the basis of work performed by McMurray and Williams [50], Rohwerder [26] suggested that SKPFM should in theory give full potential contrast for features larger than 500 nm. However, in practice even features *ca.* 2 μm in width may not provide this [26]. For example, Bengtsson Blücher *et al.* measured a potential difference of *ca.* 70 mV between an aluminium matrix and Al inclusions of ca. 2 μm in width at 85% RH using SKPFM whereas they found SKP yielded a potential difference between pure Mg and pure Al of 600 mV at the same RH [38].

Conclusions

Careful optimisation of SKPFM in terms of setting the correct drive phase prior to each measurement with a new tip allows, in the case of 99.99% pure Zn, Fe, Cu, Ni and Ag surfaces, a measurement of Volta potential differences (E_{skpfm}) which are of effectively equal magnitude to those measured using conventional SKP (E_{skp}). A good correlation between inverted E_{skpfm} values and E_{kp} has been demonstrated in the presence of a thin aqueous humidity layer formed through water adsorption at the metal surface from air at 80% RH both in the presence and absence of electrolyte dosing in that humidity layer. By exploiting the observed correlation and using a SKP which has been previously calibrated versus a series of metal/aqueous metal ion redox couples it is possible to indirectly calibrate atmospheric SKPFM in terms of electrochemical potential. However, a good correlation has also been demonstrated between atmospheric E_{kp} in the presence of a NaCl dosed humidity layer and immersion E_{corr} in sodium chloride electrolyte. This implies that SKPFM may be calibrated directly against immersion E_{corr} provided E_{skpfm} measurements are

performed under controlled and suitable conditions of atmospheric RH and surface electrolyte dosing. It is anticipated that SKPFM calibration will enhance the usefulness of this technique for atmospheric corrosion studies of metals under thin electrolyte layers and/or in the presence of ultra thin humidity induced moisture layers.

Acknowledgements

This work was performed in part under the DIAMOND ("Decommissioning, Immobilization and Management of Nuclear Wastes for Disposal") consortium project. We are therefore grateful to EPSRC for the funding of Tony Cook under grant number EP/F055412/1.

References

[1] M. Stratmann, H. Streckel, Ber. Bunsenges. Phys. Chem. 92 (1988) 1274.

[2] M. Stratmann, H. Streckel. Corros. Sci. 30 (1990) 681.

[3] M. Stratmann, H. Streckel. Corros. Sci. 30 (1990) 697.

[4] M. Stratmann, H. Streckel, K.T. Kim, S. Crockett, Corros. Sci. 30 (1990) 715.

[5] A. Leng, M. Stratmann, Corros. Sci. 34 (1993) 1657.

[6] C. Chen, F. Mansfeld, Corros. Sci. 39 (1997) 409.

[7] M. Stratmann, H. Streckel, R. Feser, Corros. Sci. 32 (1991) 467.

[8] M. Stratmann, R. Feser, A. Leng, Electrochim. Acta 39 (1994) 1207.

[9] W. Furbeth, M. Stratmann, Fresenius, J. Anal. Chem. 353 (1995) 337.

[10] A. Leng, H. Streckel, M. Stratmann, Corros. Sci. 41 (1999) 547.

[11] A. Leng, H. Streckel M. Stratmann, Corros. Sci. 41 (1999) 579.

[12] W. Furbeth, M. Stratmann, Prog. Org. Coat. 39 (2000) 23.

[13] G. Williams, H. N. McMurray, J. Electrochem Soc. 148 (2001) B337.

[14] H. N. McMurray, G. Williams, S. O'Driscoll, J. Electrochem. Soc. 151 (2004) B404.

[15] G. Williams, H.N. McMurray, D.A. Worsley, J. Electrochem. Soc. 149 (2002) B154.

[16] G. Williams, H.N. McMurray, M.J. Loveridge, Electrochim. Acta. 55 (2010) 1740.

[17] G. Williams, H.N. McMurray, Electrochem. Solid-State Lett. 6 (2003) B9.

[18] H.N. McMurray, G. Williams, Corrosion 60 (2004) 219.

[19] G. Williams, H.N. McMurray, Electrochem. Solid-State Lett. 7 (2004) B13.

[20] G. Williams, R.J. Holness, H.N. McMurray, D.A. Worsley, Electrochem. Commun. 6 (2004) 549.

[21] R.J. Holness, G. Williams, H.N. McMurray, D.A. Worsley, J. Electrochem. Soc. 152 (2005) B73.

[22] G. Williams, A. Gabriel, H.N. McMurray, A.B. Cook, J. Electrochem. Soc. 153 (2006) B425.

[23] G. Williams, H.N. McMurray, Electrochim. Acta. 54 (2009) 4245.

[24] Ch. Sommerhalter, Th. Glatzel, Th.W. Matthes, A. Jager-Waldau, M.Ch. Lux-Steiner, Appl. Surf. Sci. 157 (2000) 263.

[25] H. Jacobs, H. Knapp, A. Stemmer, Rev. Sci. Instrum. 70 (1999) 1756.

[26] M. Rohwerder, F. Turcu, Electrochim. Acta. 53 (2007) 290.

[27] P. Schmutz, G.S. Frankel, J. Electrochem. Soc. 145 (1998) 2295.

[28] R.G. Buchheit, J. Electrochem. Soc. 142 (1995) 3994.

[29] J.X. Jia, A. Atrens, G. Song, T.H. Muster, Mater. Corros. 56 (2005) 468.

[30] J.H.W. de Wit, Electrochim. Acta. 49 (2004) 2841.

[31] P. Campestrini, E.P.M. van Westing, H.W. van Rooijen, J.H.W. de Wit, Corros. Sci. 42 (2000) 1853.

[32] L. Lacroix, L. Ressier, C. Blanc, G. Mankowski, J. Electrochem. Soc. 155 (2008) C131.

[33] M. Femenia, C. Canalias, J. Pan, C. Leygraf, J. Electrochem. Soc. 150 (2003) B274.

[34] N. Sathirachinda, R. Pettersson, S. Wessman, U. Kivisäkk, J. Pan, Electrochim. Acta. 56 (2011) 1792.

[35] N. Sathirachinda, R. Pettersson, J. Pan, Corros. Sci. 51 (2009) 1850.

[36] S. Mato, G. Alcalá, T.G. Woodcock, A. Gebert, J. Eckert, L. Schultz, Electrochim. Acta. 50 (2005) 2461.

[37] M. Rohwerder, E. Hornung, M. Stratmann, Electrochim. Acta. 48 (2003) 1235.

[38] D. Bengtsson Blücher, J.-E. Svensson, L.-G. Johansson, M. Rohwerder, M. Stratmann, J. Electrochem. Soc. 151 (2004) B621.

[39] K. Doblhofer, M. Cappadonia, J. Electroanal. Chem. 243 (1988) 337.

[40] R. Gomer, G. Tryson, J. Chem. Phys. 66 (1987) 4413.

[41] Veeco Support Note 322, Revision C, Section 322.6.3

[42] G. Williams, H.N. McMurray, D.A. Worsley, J. Forensic Sci. 46 (2001) 74.

[43] L. Greenspan, J. Res. NBS. 81A (1977) 89.

[44] W. Furbeth, M. Stratmann , Corros. Sci. 43 (2001) 207.

[45] H. Dafydd, D.A. Worsley, H.N. McMurray, Corros. Sci. 47 (2005) 3006

[46] R. Hausbrand, M. Stratmann, M. Rohwerder, J. Electrochem. Soc. 155 (2008) C369.

[47] Veeco Support Note 231, Revision E Section 231.9.7.

[48] Veeco Support Note 231, Revision E Section 231.9.5.

[49] Private communication, S. Lesko (Application Engineer), Veeco Instruments, Europe.

[50] H.N. McMurray, G. Williams, J. Appl. Phys. 91 (2002) 1673.

Figure Legends

Figure 1: E_{kp} ($\Delta\psi_{solution}^{probe}$) recorded as a function of distance along a series of SKP line scans for various metals in contact with a thin aqueous humidity layer in air at 80% RH. The left hand side of the figure corresponds to an area of the metal surface which has been dosed with electrolyte (NaCl, or $AgNO_3$ for Ag) and the right hand side to a non-dosed area where the humidity layer will comprise nominally pure water.

Figure 2: Plots of (i) E_{corr} plotted versus E_{kp} for $Zn/ZnCl_2$, $Fe/FeCl_2$, $Cu/CuCl_2$ and $Ag/AgNO_3$ couples (0.5 mol dm^{-3} metal ion solutions in each case) and (ii) E_{corr} determined under a 2 mm thick electrolyte layer of 5% NaCl for Zn, Fe, Cu, Ni and Ag (0.5 mol dm^{-3} $AgNO_3$ in the case of Ag) versus E_{kp} measured under a thin humidity layer dosed with the same electrolyte.

Figure 3: E_{skpfm} determined on the Multimode (MM) minus E_{skpfm} determined on the Dimension 3100 (Dim) versus AC Drive Amplitude for Fe and Zn under ambient conditions.

Figure 4: $-E_{skpfm}$ versus E_{kp} as measured on Zn, Fe, Ni, Cu and Ag in the presence of a thin aqueous humidity layer dosed with electrolyte (NaCl, or $AgNO_3$ for Ag) in air at 80% RH.

Figure 5: $-E_{skpfm}$ versus E_{kp} determined on Zn, Fe, Ni, Cu and Ag in the presence of a thin, non-dosed, aqueous humidity layer (nominally pure water) in air of 80% RH.

Figure 6: Solid symbols: data from Fig. 4 re-plotted as E_{corr} versus -E_{skpfm} for metals in the presence of a thin, electrolyte dosed, humidity layer. Open symbols: data from Fig. 5 re-plotted as E_{corr} versus -E_{skpfm} for metals in the presence of a thin, non-dosed, humidity layer (nominally pure water). The E_{kp} values of Figs 4 and 5 were converted to E_{corr} values using the calibration data presented in line (i) of Fig. 2. All measurements were carried out in air at 80%RH.

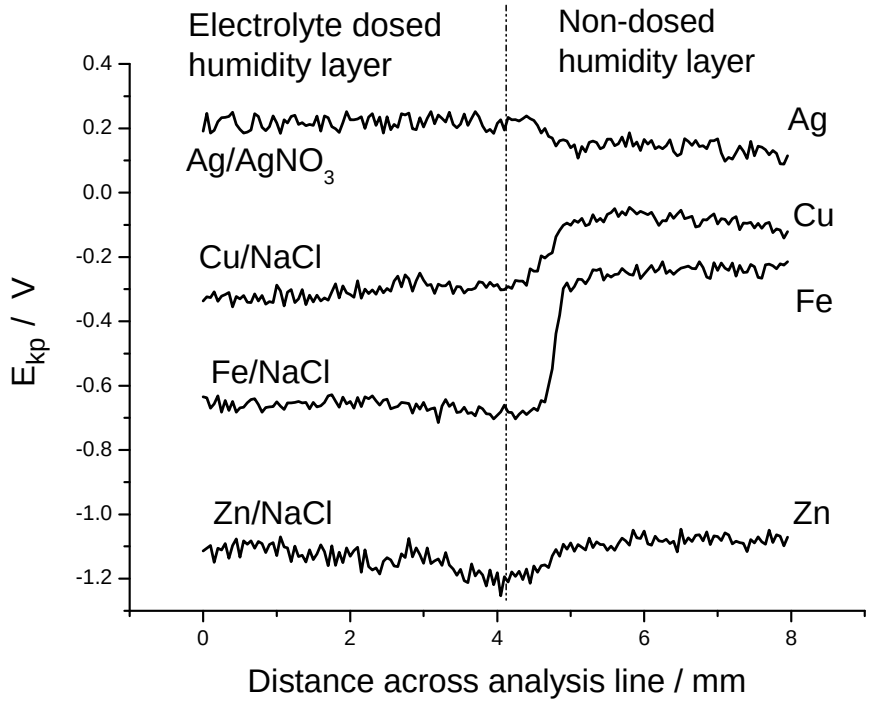

Figure 1: E_{kp} ($\Delta\psi^{probe}_{solution}$) recorded as a function of distance along a series of SKP line scans for various metals in contact with a thin aqueous humidity layer in air at 80% RH. The left hand side of the figure corresponds to an area of the metal surface which has been dosed with electrolyte (NaCl, or $AgNO_3$ for Ag) and the right hand side to a non-dosed area where the humidity layer will comprise nominally pure water.

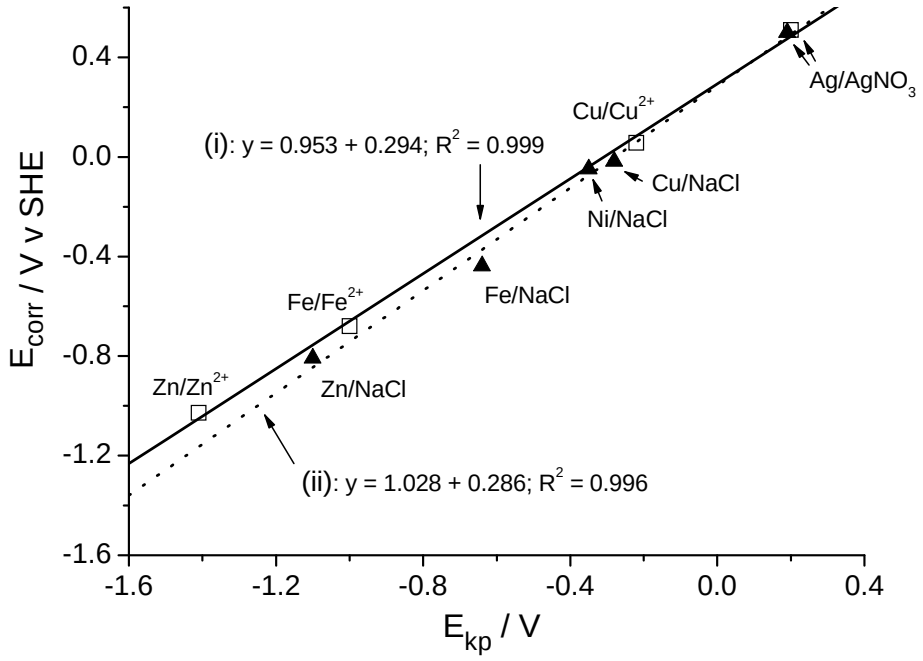

Figure 2: Plots of (i) E_{corr} plotted versus E_{kp} for $Zn/ZnCl_2$, $Fe/FeCl_2$, $Cu/CuCl_2$ and $Ag/AgNO_3$ couples (0.5 mol dm^{-3} metal ion solutions in each case) and (ii) E_{corr} determined under a 2 mm thick electrolyte layer of 5% NaCl for Zn, Fe, Cu, Ni and Ag (0.5 mol dm^{-3} $AgNO_3$ in the case of Ag) versus E_{kp} measured under a thin humidity layer dosed with the same electrolyte.

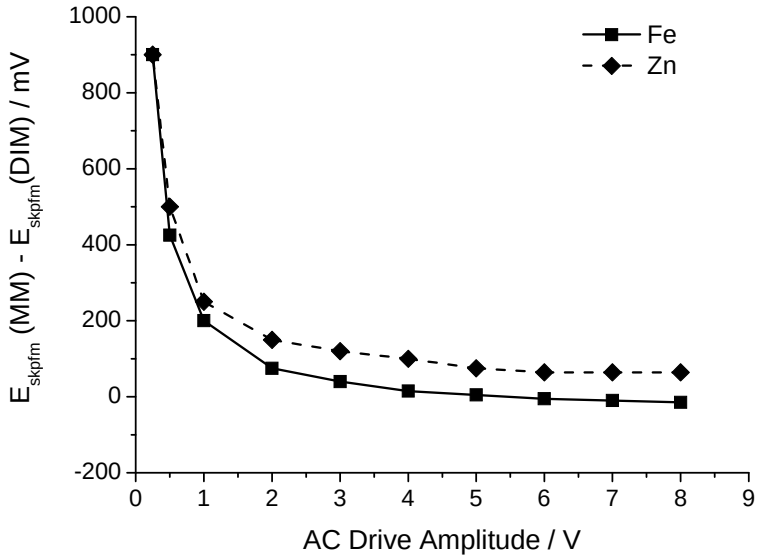

Figure 3: E_{skpfm} determined on the Multimode (MM) minus E_{skpfm} determined on the Dimension 3100 (Dim) versus AC Drive Amplitude for Fe and Zn under ambient conditions.

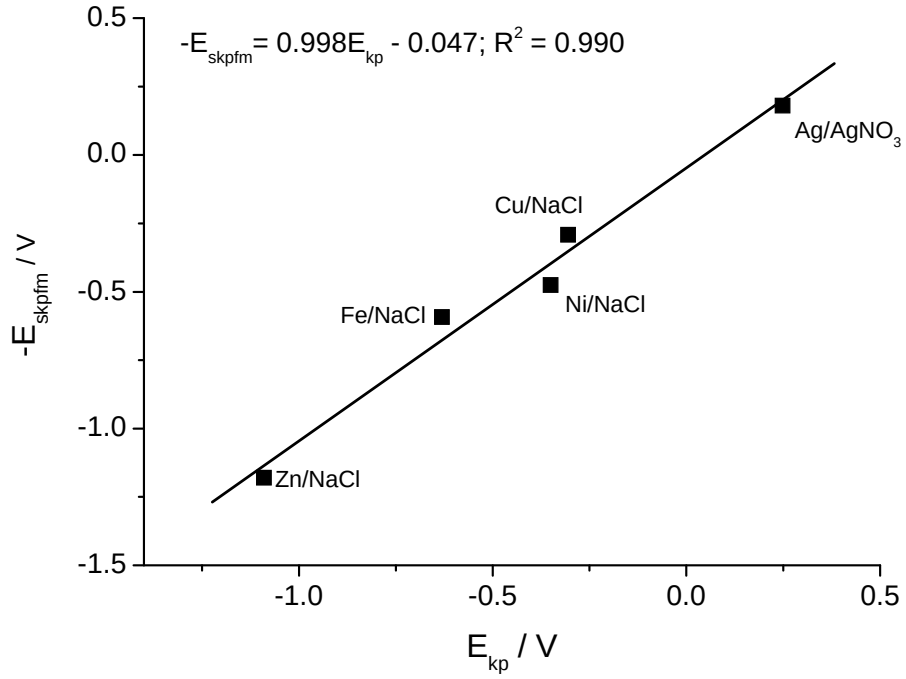

Figure 4: -E_{skpfm} versus E_{kp} as measured on Zn, Fe, Ni, Cu and Ag in the presence of a thin aqueous humidity layer dosed with electrolyte (NaCl, or $AgNO_3$ for Ag) in air at 80% RH.

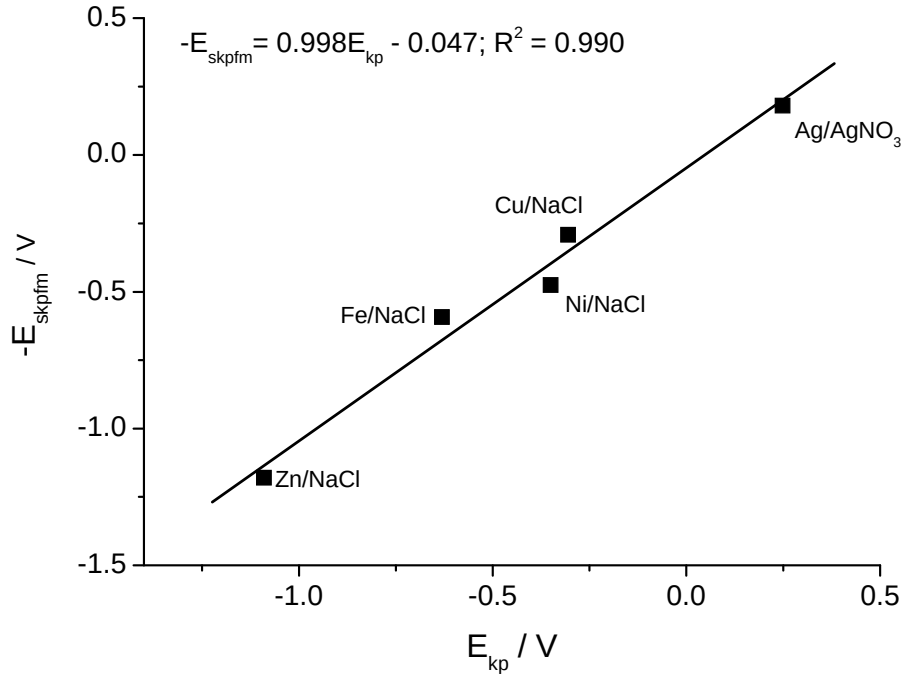

Figure 5: -E_{skpfm} versus E_{kp} determined on Zn, Fe, Ni, Cu and Ag in the presence of a thin, non-dosed, aqueous humidity layer (nominally pure water) in air of 80% RH.

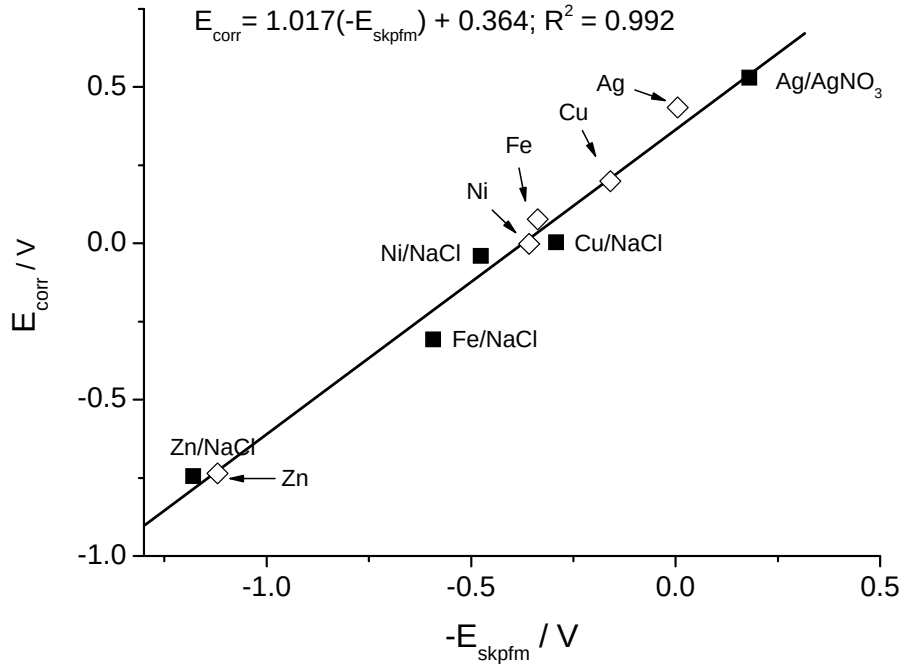

Figure 6: Solid symbols: data from Fig. 4 re-plotted as E_{corr} versus $-E_{skpfm}$ for metals in the presence of a thin, electrolyte dosed, humidity layer. Open symbols: data from Fig. 5 re-plotted as E_{corr} versus $-E_{skpfm}$ for metals in the presence of a thin, non-dosed, humidity layer (nominally pure water). The E_{kp} values of Figs 4 and 5 were converted to E_{corr} values using the calibration data presented in line (i) of Fig. 2. All measurements were carried out in air at 80%RH.